

Intraband magnetospectroscopy of singly and doubly charged n -type self-assembled quantum dots

B. A. Carpenter,^{1,*} E. A. Zibik,¹ M. L. Sadowski,² L. R. Wilson,^{1,†} D. M. Whittaker,¹ J. W. Cockburn,¹ M. S. Skolnick,¹ M. Potemski,² M. J. Steer,³ and M. Hopkinson³

¹*Department of Physics and Astronomy, University of Sheffield, Sheffield, S3 7RH, United Kingdom*

²*Grenoble High Magnetic Field Laboratory, CNRS, Grenoble, France*

³*EPSRC National Centre for III-V Technologies, Sheffield, S1 3JD, United Kingdom*

(Received 3 August 2006; published 13 October 2006)

The influence of quantum dot occupancy and incident light polarization on the carrier-lattice interactions in electron-doped InAs quantum dots grown on GaAs has been investigated up to 28 T by far-infrared magnetotransmission spectroscopy. An enhancement of the electron-phonon coupling with increased electron population from one to two electrons per dot is observed, in close agreement with the predicted $\sqrt{2}$ increase due to the antisymmetrization of the electron wave function in the two-electron quantum dot system. This contrasts with two-dimensional systems in which the polaron coupling strength is reduced with increasing electron density due to the screening effect of multiple carriers on the electron-phonon interaction. A clear change of the polarization dependence for transitions from the ground to the first excited state from linear to circular has been observed as the Zeeman splitting becomes larger than the zero-field excited state splitting energy.

DOI: [10.1103/PhysRevB.74.161302](https://doi.org/10.1103/PhysRevB.74.161302)

PACS number(s): 73.21.La, 71.55.Eq, 71.38.Mx

The last decade has seen considerable investigations into the properties of quantum dots (QDs) which continue to provide interest through their inherent three-dimensional confinement and discrete density of states. In QDs the interaction between the carriers and phonons promotes the formation of a metastable quasiparticle known as the polaron.¹⁻⁵ Magnetotransmission measurements performed on n - (Ref. 6) and p -type⁷ self-assembled InAs/GaAs QD structures have demonstrated clear evidence for the polaron picture with strong anticrossings observed close to multiple longitudinal-optical (LO) phonon energies. The formation of polarons has significant implications for carrier relaxation processes in QDs as already reported.^{8,9}

We present polarization-dependent, far-infrared magnetotransmission measurements of polarons in InAs/GaAs self-assembled quantum dots with applied magnetic fields up to 28 T. From our measurements of samples doped to contain either one (sample I) or two (sample II) electrons per dot we observe an enhancement of the coupling between the mixed electron-LO-phonon states with increased carrier population. Polarization-dependent measurements show an almost complete change from linear to circular polarization for intersublevel transitions with increasing magnetic field.

The InAs/GaAs QD samples were grown on (100) GaAs substrates by molecular beam epitaxy in the Stranski-Krastanow mode and contain 80 layers of InAs QDs separated by 50 nm intrinsic GaAs spacers. Prior to growth of the multilayer samples, uncapped reference samples were grown from which we were able to determine the QD density per layer (typically $\sim 4 \times 10^{10} \text{ cm}^{-2}$) from atomic force microscope analysis. In order to achieve average populations of one (two) electron(s) per dot the multilayer samples were doped in the GaAs barrier 2 nm below the QD layers with a sheet density equal to (or twice) the measured dot density. The linewidth of the transmission in these samples compares well with detailed studies of 20-layer samples¹⁰ indicating high uniformity of the carrier density for the 80-layer QD

stacks studied here. The far-infrared transmission was measured with a Fourier transform spectrometer coupled to a resistive 28 T magnet by means of light pipe optics. A silicon bolometer placed directly below the sample was used to detect the transmitted radiation. Spectra were normalized using the transmission of an identical but undoped reference sample at each magnetic field.

The measured transitions occur between the electron ground ($|s\rangle$) and first excited ($|p\rangle$) states, the latter of which is split into two levels $|p_{-}\rangle$ and $|p_{+}\rangle$ due to dot anisotropy.¹¹ If only the QD shape symmetry is taken into account, the dots are assumed to have cylindrical symmetry $C_{\infty v}$ giving a two-fold degenerate p level with total angular momentum $M_{\text{total}} = \pm 1$,¹² and no optical polarization anisotropy in the (001) plane, in which case the s to p state transition will be unpolarized. However, due to possible elongation of the QD along the $[0\bar{1}1]$ direction,¹³ and also strain-induced piezoelectric¹⁴ and atomistic relaxation¹⁵ effects, the real QD symmetry is reduced to C_{2v} . In this symmetry group the first excited state is nondegenerate and splits into two p_{-} and p_{+} sublevels with M_{total} of either $(1/\sqrt{2})(|+\rangle+|-\rangle)$ or $(1/\sqrt{2})(|+\rangle-|-\rangle)$. This leads to two oppositely polarized allowed transitions between s and p states oriented perpendicular and parallel to the $\langle 011 \rangle$ crystal axis.

Figure 1 shows the transmission spectra in the Faraday geometry at various magnetic fields for sample I, where the magnetic field is normal to the QD layers. The anisotropy splitting of the p states at zero field is clearly visible. The 15% transmission due to the 80-layer samples allows clear observation of the anticrossings that are the clear signatures of polaron formation. With increasing magnetic field, these peaks shift apart due to the Zeeman effect and display anti-crossing behavior when close to resonance with an integer multiple of the LO-phonon energy.

Figure 2 shows the intersublevel states involved and their respective dispersion with magnetic field. These $|\text{electron, phonon}\rangle$ states provide the basis for the diagonal-

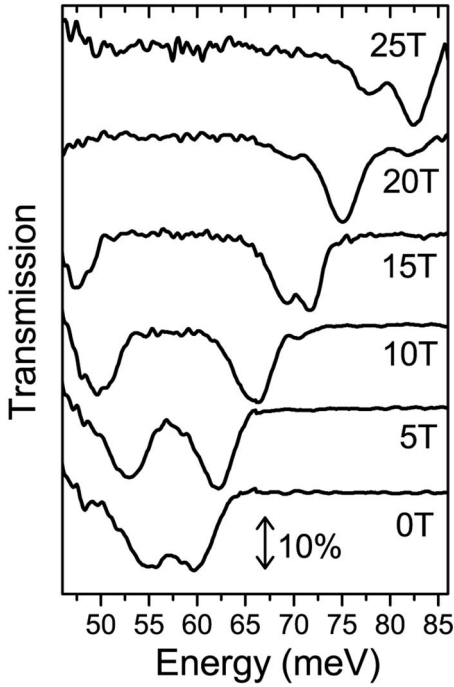


FIG. 1. Unpolarized normal incidence transmission through sample I for various magnetic fields. The zero-field splitting is clearly visible, as are the anticrossings characteristic of a polaronic system near to 15 and 25 T.

ization of the Fröhlich Hamiltonian ($\hat{\mathcal{H}}_{\text{int}}^i$) which describes the QD electron-phonon interaction:

$$|s, n\rangle = n \times E_{\text{LO}}, \quad (1)$$

$$|p_{\pm}, n\rangle = E_p(0) \pm \frac{1}{2} \hbar \omega_c + \gamma B^2 + n \times E_{\text{LO}}, \quad (2)$$

where s and p_{\pm} are the s and p eigenstates of $\hat{\mathcal{H}}_{\text{int}}^i$, n is the number of phonons, and $\omega_c = eB/m^*$ is the cyclotron frequency induced by the magnetic field. The zero of energy is taken to be the $|s, 0\rangle$ state.

Fröhlich interactions occur strongly between states differing by one phonon. Thus only those transitions involving a change of one in the phonon number between initial and final states are coupled, as given by Eqs. (3) and (4).

$$\langle p_{\pm}, m | \hat{\mathcal{H}}_{\text{int}}^{(i)} | s, n \rangle = \phi_{p_{\pm}}(r_i) \hat{\mathcal{H}}_{\text{int}}^{(i)} \phi_s(r_i) = V_{sp_{\pm}}, \quad (3)$$

$$\langle p_{\pm}, m | \hat{\mathcal{H}}_{\text{int}}^{(i)} | p_{\mp}, n \rangle = \phi_{p_{\pm}}(r_i) \hat{\mathcal{H}}_{\text{int}}^{(i)} \phi_{p_{\mp}}(r_i) = V_{p_{\pm}p_{\mp}}. \quad (4)$$

Each $\hat{\mathcal{H}}_{\text{int}}^{(i)}$ acts on a single electron i arising from the separable nature of $\hat{\mathcal{H}}_{\text{int}}^i$ as a single-particle operator. The phonon number $m = n \pm 1$ where $n = 1, 2$.

In Fig. 2, at each of the points where two basis states that differ by one phonon cross, an anticrossing is seen in the experimental data. At low energy, the anticrossing occurs between the states $|s, 1\rangle$ and $|p_{-}, 0\rangle$. The magnitude of this coupling is found by fitting the field variation of the observed polaron branch using its deviation from the $|p_{-}, 0\rangle$

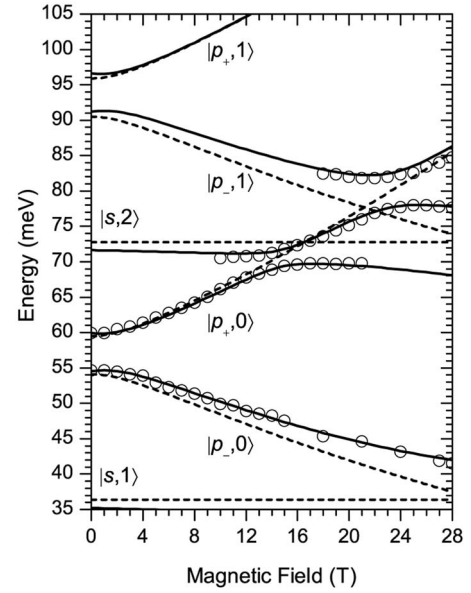


FIG. 2. Variation of the conduction band |electron, phonon> basis states with magnetic field. The electron component is labeled in accordance with atomic orbitals; the phonon component is given as a whole number of LO phonons. The splitting at zero field arises from the anisotropy of the wave functions. Open circles show experimental results for sample I; solid lines show the fit; dashed lines show the basis states described in Eqs. (1) and (2) used to generate the fit.

state. Anticrossings also occur around 15 T (70 meV) and 23 T (80 meV) from interactions between the states $|p_{+}, 0\rangle$, $|p_{-}, 1\rangle$, and $|s, 2\rangle$. The interaction between the $|p_{-}, 1\rangle$ and $|p_{+}, 0\rangle$ states at 23 T (80 meV) results in the anticrossing between the $|p_{+}, 0\rangle$ and $|s, 2\rangle$ states occurring below the $|s, 2\rangle$ energy. The solid lines represent the fit to sample I, using $\langle p_{-}, 0 | \hat{\mathcal{H}}_{\text{int}} | s, 1 \rangle = 5.2$ meV.

In the two-electron system (sample II) the ground and first excited states can be represented by the following antisymmetric spin singlets, using the separable nature of the Fröhlich Hamiltonian acting on this system:

$$|ss\rangle = \frac{1}{\sqrt{2}} (|\uparrow, \downarrow\rangle - |\downarrow, \uparrow\rangle) \phi_s(r_1) \phi_s(r_2), \quad (5)$$

$$|sp_{\pm}\rangle = \frac{1}{\sqrt{2}} (|\uparrow, \downarrow\rangle - |\downarrow, \uparrow\rangle) \times \frac{1}{\sqrt{2}} [\phi_s(r_1) \phi_{p_{\pm}}(r_2) + \phi_s(r_2) \phi_{p_{\pm}}(r_1)]. \quad (6)$$

Applying $\hat{\mathcal{H}}_{\text{int}}^i$ to the |two-electron, phonon> state $|ss, 1\rangle$ coupled to $|sp_{-}, 0\rangle$ gives an enhancement by a factor of $\sqrt{2}$ as a consequence of the antisymmetrization of the two-particle wave function:¹⁶

$$\langle sp_{-} | \hat{\mathcal{H}}_{\text{int}} | ss \rangle = \langle sp_{-} | \hat{\mathcal{H}}_{\text{int}}^{(1)} + \hat{\mathcal{H}}_{\text{int}}^{(2)} | ss \rangle = \sqrt{2} V_{sp_{-}}. \quad (7)$$

The phonon components are left out of the above equation for simplicity; it is necessary that these two-electron states

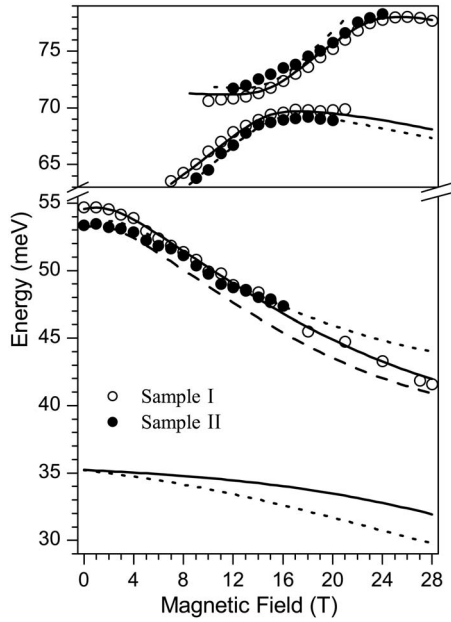


FIG. 3. Variation of the normal incidence absorption peaks with applied magnetic field in the Faraday geometry. Solid (dotted) lines represent the fit to sample I (II). The dashed line attempts to fit to sample II using the parameters from sample I, but with a lower-energy zero-field value. The lower (upper) part of the figure corresponds to transitions from the electron ground state s to the polaron states involving the p_- (p_+) electron excited state.

differ by one phonon for them to interact strongly.

Figure 3 shows the experimental points for both samples. The dashed line in the lower part of Fig. 3 is the fit to sample I shifted to lower energy by 1.3 meV to give the best fit at $B=0$ to sample II, but resulting in a poor fit at higher fields. The interaction strength $\langle p_-, 0 | \hat{\mathcal{H}}_{\text{int}} | s, 1 \rangle = V_{sp_-}$ is then multiplied by $\sqrt{2}$ as predicted in Eq. (7) caused by the presence of a spectator s electron. The fit from using this procedure is shown by the dotted line in the lower part of Fig. 3 and gives good agreement with the experimental points for sample II. This enhancement in the interaction energies is in contrast to two-dimensional systems, in which the polaron coupling strength is reduced with increasing electron density due to the screening effect of multiple carriers on the electron-phonon interaction.¹⁷

Further evidence for the increase of the electron-phonon interaction strength for two electrons compared to the one-electron case can be seen in the upper part of Fig. 3, where the anticrossing at ~ 70 meV for both samples is shown. This anticrossing occurs from the interaction between the states $|s, 2\rangle$, $|p_+, 0\rangle$, and $|p_-, 1\rangle$. The Fröhlich Hamiltonian only couples strongly states that differ by one phonon and the coupling of states differing by two or more phonons is very weak, implying that the anticrossing between the states $|s, 2\rangle$ and $|p_+, 0\rangle$ should not be observable. It is the combined interactions of the states $|p_+, 0\rangle$ with $|p_-, 1\rangle$ and $|s, 2\rangle$ with $|p_-, 1\rangle$ that permit these states to interact strongly. These interactions occur in the region shown by the upper part of Fig. 3 and are best summarized by the matrix used to achieve the good fits in the figures:

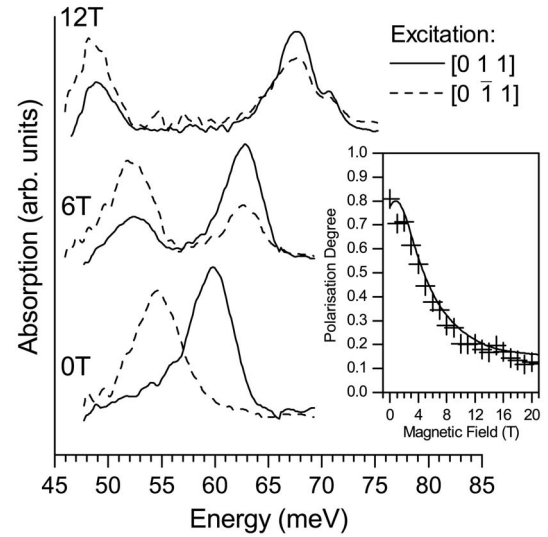


FIG. 4. Variation of the linearly polarized absorption spectra with magnetic field, for sample I. The inset shows variation of the degree of linear polarization for the $|s\rangle \rightarrow |p_+, 0\rangle$ transition (+ symbols) in the energy range 57–70 meV with the fit obtained from the model (solid line).

$$\begin{pmatrix} E_{p_+}(B) & 0 & V_{p_+p_-} \\ 0 & 2E_{\text{LO}} & V_{sp_-} \\ V_{p_+p_-}^* & V_{sp_-}^* & E_{p_-}(B) + E_{\text{LO}} \end{pmatrix}. \quad (8)$$

Notice that the direct interaction term is zero between the states $|p_+, 0\rangle$ and $|s, 2\rangle$ that have energies $E_{p_+}(B)$ and $2E_{\text{LO}}$, respectively.

The eigenvalues give the magnitude of the discussed anticrossing to be directly proportional to the product of the interaction energies $V_{p_+p_-}$ and V_{sp_-} . The increased anticrossing magnitude for sample II over sample I shown clearly in the upper part of Fig. 3 can now be explained. It is directly proportional to the interaction energy V_{sp_-} which is enhanced by a factor of $\sqrt{2}$ over the one-electron system. Measurements of the anticrossing magnitude in the upper part of Fig. 3 show 2.8 ± 0.2 meV for sample I, increasing to 4.0 ± 0.4 meV for sample II. The ratio of these values (1.5 ± 0.2) agrees well with the predicted $\sqrt{2}$ increase.

The magnetic field dependence of the linear polarization was investigated using polythene wire grid polarizers attached directly to the surface of the samples. Linearly polarized magnetotransmission spectra for sample I at fields of 0, 6, and 12 T are shown in Fig. 4. At zero magnetic field we observe two absorption peaks linearly polarized in the $[0\bar{1}1]$ and $[011]$ directions. As can be seen, with applied external magnetic field the degree of linear polarization of the absorption peaks is diminished. The inset shows the degree of linear polarization defined as the modulus of the difference between the absorption resonance amplitudes divided by their sum. At zero magnetic field the polarization degree for s to p transitions is about 0.8. The small departure from a polarization degree of unity probably arises because the inhomogeneous broadening of the intersublevel absorption peaks

(~ 5 meV) due to the QD size variation across the wafer is comparable to the p -state splitting, making it difficult to determine correctly the polarization degree at zero magnetic field. The eigenvector data from the same model used earlier to successfully fit the resonance peaks is used here to model the trend in the linear polarization degree. A polarization degree of unity is predicted at zero field by the model (as expected) and this fit is then scaled to match the zero-field value of about 0.8 observed experimentally, giving the good fit shown in Fig. 4 (inset) for all magnetic fields. There is a clear reduction in the degree of linear polarization with increasing magnetic field as the Zeeman splitting becomes comparable to or larger than the zero-field splitting energy. This is analogous to the situation for interband transitions in quantum dots where excitons are linearly polarized initially due to the fine structure splitting and become circularly polarized in magnetic fields.¹⁸ The clear decrease of linear polarization with increasing magnetic field is a satisfactory demonstration that the p states are decoupled from the linear combination $(1/\sqrt{2})(|+\rangle \pm |-\rangle)$ at $B=0$ to pure $|+\rangle$ and $|-\rangle$

states when the magnetic-field-induced Zeeman splitting becomes greater than the zero-field p state splitting energy.

In conclusion, we have used far-infrared magnetotransmission measurements to investigate the effects of quantum dot electron population on the electron-phonon interaction. We find an enhancement of the electron-phonon coupling with increased electron population from one to two electrons per dot, in good agreement with the predicted $\sqrt{2}$ increase due to the antisymmetrization of the electron wave function in the two-electron quantum dot system. Furthermore, by studying the polarization dependence for ground to first excited state transitions as a function of magnetic field, we observe a clear change from linear to circular polarization as the Zeeman splitting becomes larger than the zero-field excited state splitting energy.

Financial support provided by the U.K. Engineering and Physical Sciences Research Council (EPSRC) under Grants No. GR/S76076/01 and No. GR/T21158/01 is gratefully acknowledged.

*Electronic address: b.carpenter@sheffield.ac.uk

†Electronic address: luke.wilson@sheffield.ac.uk

¹X.-Q. Li and Y. Arakawa, Phys. Rev. B **57**, 12285 (1998).

²S. Hameau, Y. Guldner, O. Verzellen, R. Ferreira, G. Bastard, J. Zeman, A. Lemaître, and J. M. Gérard, Phys. Rev. Lett. **83**, 4152 (1999).

³L. Jacak, J. Krasnyj, D. Jacak, and P. Machnikowski, Phys. Rev. B **67**, 035303 (2003).

⁴V. Preisler, T. Grange, R. Ferreira, L. A. de Vaulchier, Y. Guldner, F. J. Teran, M. Potemski, and A. Lemaître, Phys. Rev. B **73**, 075320 (2006).

⁵B. Aslan, H. C. Liu, M. Korkusinski, P. Hawrylak, and D. J. Lockwood, Phys. Rev. B **73**, 233311 (2006).

⁶S. Hameau, J. N. Isaia, Y. Guldner, E. Deleporte, O. Verzellen, R. Ferreira, G. Bastard, J. Zeman, and J. M. Gérard, Phys. Rev. B **65**, 085316 (2002).

⁷V. Preisler, R. Ferreira, S. Hameau, L. A. de Vaulchier, Y. Guldner, M. L. Sadowski, and A. Lemaître, Phys. Rev. B **72**, 115309 (2005).

⁸E. A. Zibik *et al.*, Phys. Rev. B **70**, 161305(R) (2004).

⁹S. Sauvage, P. Boucaud, R. P. S. M. Lobo, F. Bras, G. Fishman, R.

Prazeres, F. Glotin, J. M. Ortega, and J.-M. Gérard, Phys. Rev. Lett. **88**, 177402 (2002).

¹⁰J. N. Isaia, L. A. de Vaulchier, S. Hameau, R. Ferreira, Y. Guldner, E. Deleporte, J. Zeman, V. Thierry-Mieg, and J.-M. Gérard, Eur. Phys. J. B **35**, 209 (2003).

¹¹G. Bester and A. Zunger, Phys. Rev. B **71**, 045318 (2005).

¹²A. Wojs and P. Hawrylak, Phys. Rev. B **53**, 10841 (1996).

¹³P. B. Joyce, T. J. Krzyzewski, G. R. Bell, and T. S. Jones, Appl. Phys. Lett. **79**, 3615 (2001).

¹⁴O. Stier, M. Grundmann, and D. Bimberg, Phys. Rev. B **59**, 5688 (1999).

¹⁵G. Bester, S. Nair, and A. Zunger, Phys. Rev. B **67**, 161306(R) (2003).

¹⁶O. Verzellen, Ph.D. thesis, Université Paris VI, 2002.

¹⁷F. M. Peeters, X.-G. Wu, J. T. Devreese, C. J. G. M. Langerak, J. Singleton, D. J. Barnes, and R. J. Nicholas, Phys. Rev. B **45**, 4296 (1992).

¹⁸V. D. Kulakovskii, G. Bacher, R. Weigand, T. Kümmell, A. Forchel, E. Borovitskaya, K. Leonardi, and D. Hommel, Phys. Rev. Lett. **82**, 1780 (1999).